

# Organ-Level Histological and Biomechanical Responses from Localized Osteoarticular Injury in the Rabbit Knee

Tanawat Vaseenon,<sup>1</sup> Yuki Tochigi,<sup>1</sup> Anneliese D. Heiner,<sup>1,2</sup> Jessica E. Goetz,<sup>1,2</sup> Thomas E. Baer,<sup>1</sup> Douglas C. Fredericks,<sup>1</sup> James A. Martin,<sup>1,2</sup> M. James Rudert,<sup>1</sup> Stephen L. Hillis,<sup>3,4</sup> Thomas D. Brown,<sup>1,2</sup> Todd O. McKinley<sup>1</sup>

<sup>1</sup>Department of Orthopaedics and Rehabilitation, University of Iowa, Iowa City, Iowa, <sup>2</sup>Department of Biomedical Engineering, University of Iowa, Iowa City, Iowa, <sup>3</sup>Center for Research in the Implementation of Innovative Strategies in Practice (CRIISP), VA Iowa City Medical Center, Iowa City, Iowa, <sup>4</sup>Department of Biostatistics, University of Iowa, Iowa City, Iowa

Received 29 March 2010; accepted 13 August 2010

Published online in Wiley Online Library (wileyonlinelibrary.com). DOI 10.1002/jor.21259

**ABSTRACT:** The processes of whole-joint osteoarthritis development following localized joint injuries are not well understood. To demonstrate this local-to-global linkage, we hypothesized that a localized osteoarticular injury in the rabbit knee would not only cause biomechanical and histological abnormalities in the involved compartment but also concurrent histological changes in the noninvolved compartment. Twenty rabbits had an acute osteoarticular injury that involved localized joint incongruity (a 2-mm osteochondral defect created in the weight-bearing area of the medial femoral condyle), while another 20 received control sham surgery. At the time of euthanasia at 8 or 16 weeks post-surgery, the experimental knees were subjected to sagittal-plane laxity measurement, followed by cartilage histomorphological evaluation using the Mankin score. The immediate effects of defect creation on joint stability and contact mechanics were explored in concomitant rabbit cadaver experimentation. The injured animals had cartilage histological scores significantly higher than in the sham surgery group ( $p < 0.01$ ) on the medial femoral, medial tibial, and lateral femoral surfaces (predominantly on the medial surfaces), accompanied by slight (mean 20%) increase of sagittal-plane laxity. Immediate injury-associated alterations in the medial compartment contact mechanics were also demonstrated. Localized osteoarticular injury in this survival animal model resulted in global joint histological changes. © 2010 Orthopaedic Research Society. Published by Wiley Periodicals, Inc. *J Orthop Res*

**Keywords:** joint injury; osteoarthritis; cartilage histology; rabbit knee; osteochondral defect

Post-traumatic osteoarthritis (OA) manifests as progressive degeneration of the whole joint following an injury. The pathogenesis of this disorder is multifactorial,<sup>1</sup> including acute mechanical damage to the cartilage at the time of the injury, and chronic abnormal loading patterns that ensue due to decrements in articular surface congruity, stability, and alignment. While some of these injury-related factors are localized within single components of the joint, end-stage post-traumatic OA is characterized by destructive changes expanding to affect the entire joint. These observations suggest that there are organ-level mechanisms by which local articular surface injuries lead to whole-joint degeneration. However, the pathomechanisms responsible for disease progression to organ level have not been well documented.

It has long been accepted that articular surface incongruity results in local cartilage over-loading that leads to degeneration. However, laboratory experiments in static cadaveric preparations documented only modest increases in cartilage contact stresses in the face of substantial incongruities.<sup>2,3</sup> Dynamically, in cadaveric preparations of incongruous joints subjected to a physiologic motion/load sequence, although the increase in contact stresses was modest, several-fold increases in local cartilage loading rates were demonstrated.<sup>4,5</sup> These observations imply that incongruity presumably causes pathogenic dynamic aberrations in local joint contact mechanics as well as in whole-joint kinematics. This dynamic mechanism may be an important co-factor that

contributes to progression of whole-joint cartilage degeneration from a localized osteoarticular injury.

This study was designed to investigate *in vivo* the association between localized osteoarticular injury and whole-joint OA development. In a survival animal experiment, an osteochondral defect in the primary weight-bearing region of the medial femoral condyle was created in the rabbit knee, and the whole-organ short-to-mid-term effects were explored. The immediate biomechanical effects of the defect creation were also studied in concomitant rabbit knee cadaver experiments. The hypothesis was that a localized osteoarticular injury in the medial femoral primary weight-bearing surface would cause whole-joint cartilage degeneration, along with biomechanical abnormalities that plausibly explain the disease progression.

## METHODS

### Survival Experimentation

Forty mature New Zealand white rabbits (12–15 months old, average weight 4.5 kg) were subjected to surgery in the left knee. Surgery was performed under general anesthesia, with the animal in the prone position, to approach the primary contact region of the medial femoral condyle at 135° of flexion (representative habitual knee position for rabbits placed in cage confinement<sup>6,7</sup>) (Fig. 1). A medial popliteal longitudinal skin incision was made, and the posteromedial joint capsule was exposed through the intermuscular plane between the semimembranosus and medial gastrocnemius. The gastrocnemius tendon was retracted laterally, with the femoral insertion left intact. The joint capsule was then incised longitudinally. In 20 animals, a circular osteochondral defect that reached sub-chondral bone, typically 1–1.5 mm depth, was created at the center of the posterior femoral surface (the incongruous injury group). Using a 2-mm dermal biopsy punch, cartilage and bone in a sharp circular cut were

Correspondence to: Yuki Tochigi (T: 319-335-7547; F: 319-335-7530; E-mail: yuki-tochigi@uiowa.edu)

© 2010 Orthopaedic Research Society. Published by Wiley Periodicals, Inc.

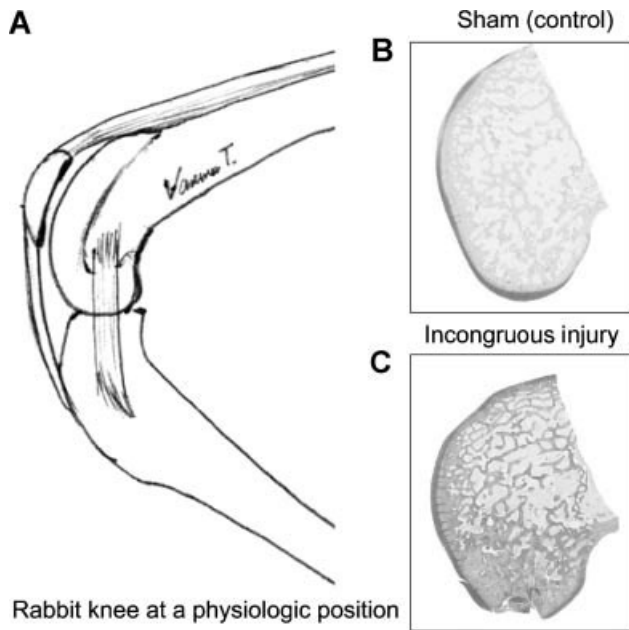


**Figure 1.** (A) The habitual physiologic knee position for rabbits in cage confinement is about  $135^\circ$  of flexion. (B and C) Histological findings at the time of euthanasia indicated that the defect was created at a region where articular cartilage was thickest.

simultaneously removed (like harvesting a cylindrical osteochondral allograft). The other 20 animals received the posterior arthrotomy alone (the sham surgery control group). All animals were allowed free cage activity and an ad lib diet. For each treatment group, half of the animals were sacrificed at 8 weeks, and the other half at 16 weeks. The surgery, euthanasia, and other animal care protocols were approved by the Institutional Animal Care and Use Committee.

At euthanasia, the experimental knees were subjected to sagittal-plane stability measurement using a custom loading fixture designed for the rabbit knee<sup>8</sup> (Fig. 2A). In this device, the rabbit was placed in the supine position, with the femur secured vertically using percutaneous half-pins. The tibia was secured with transverse pins to a horizontal leg holder, with the knee held at  $90^\circ$  flexion. The leg holder was in turn attached to a stepper-motor-driven actuator. The actuator applied cyclic anterior and posterior knee drawer displacement at a test speed of 1 mm/s, with limits for direction reversal set as  $\pm 75$  N or  $\pm 3$  mm, whichever was reached first. Force-versus-displacement data were continuously recorded. The test sequence consisted of four discrete preconditioning cycles (during which the “zero” displacement position was adjusted), followed by four cycles of preconditioning, and then four loading cycles for data collection. The knee drawer force-versus-displacement relationship was typically characterized by a sigmoid curve (Fig. 2B). The length of the central flat portion of the curve, within the range of  $\pm 7.5$  N of drawer force, was defined as the neutral-zone length (NZL). The NZL data for each of the four data collection cycles were averaged.

The experimental knees were then prepared for cartilage histological evaluation, following OARSI guidelines.<sup>9</sup> For each joint, sagittal sections (stained with Safranin O-Fast Green) were created for the medial/lateral femoral condyles and the medial/lateral tibial plateaus. High magnification digital images were then captured at 743,028 pixels/mm<sup>2</sup> resolution, using a QICAM<sup>®</sup> 12-bit camera (QImaging<sup>™</sup>, Surrey, BC, Canada) mounted on a microscope (Model BX60, Olympus Co., Tokyo, Japan) with a  $4\times$  objective, coupled with a stepper-

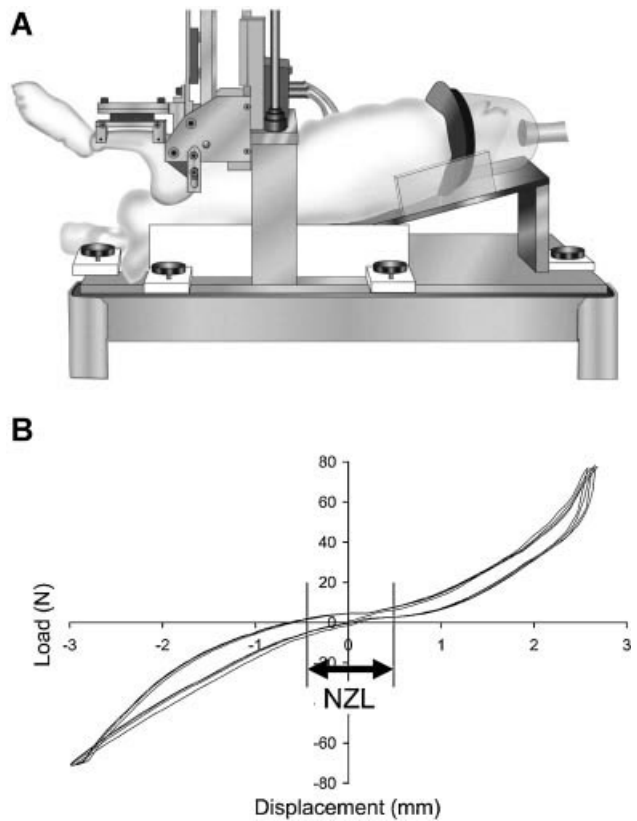


**Figure 2.** (A) Custom loading fixture for the sagittal-plane stability test (reprinted from Ref.<sup>8</sup>). (B) Definition of the neutral-zone length (NZL: displacement between  $\pm 7.5$  N) from the load–displacement relationship.

motor-driven stage (Prior Scientific, Inc., Rockland, MD). Individual high-resolution image fields were concatenated using Image-Pro<sup>®</sup> (Media Cybernetics, Inc., Silver Spring, MD) to produce (stitched) full-cartilage-thickness osteochondral images. For each section, the central part (about 1 mm wide) of the joint surface’s primary weight-bearing region (where cartilage was thickest) was cropped, and a unique identification number was randomly assigned. In the case of medial femoral sections for the incongruous injury group, a representative region adjacent to the surgically created defect (either anterior or posterior, at least 0.5 mm away from the defect edge) was selected. Cartilage histology was evaluated in a blinded fashion using Mankin’s Histological Histochemical Grading Scale (HHGS).<sup>10</sup> The femoral and tibial surfaces in the medial and lateral compartments were rated individually. Two experienced orthopedic surgeons (T.V. and Y.T.) rated these blinded images. Each observer individually scored each image twice (i.e., a total of 4 scores per image), and the mean value was recorded.

#### Cadaver Experimentation

The immediate effects of the same osteoarticular injury on contact mechanics were assessed in seven fresh rabbit cadaver knees. These specimens were dissected free of skin and surrounding tissue, with the major ligaments and menisci left intact. The distal femur and proximal tibia were potted into separate PMMA blocks, with the knee held at about  $135^\circ$  of flexion. The specimen was then mounted in a custom-designed loading device (Fig. 3A) actuated by an electromechanical materials testing machine (MTS Insight 1, MTS Systems Corp., Eden Prairie, MN). Knee flexion/extension was adjust-

able in  $5^\circ$  increments. Ad/abduction about the axis aligned with the knee center was left unrestricted, allowing the joint to align naturally while the load was applied. To measure contact stresses in the medial compartment, a  $10\text{ mm} \times 30\text{ mm}$  rectangle pressure sensitive film (Low Range Prescale<sup>®</sup>, Fujifilm Co., Tokyo, Japan) was inserted into the knee beneath the meniscus, through a small arthrotomy. Axial compression was linearly increased over 2 s to a physiologic-level force<sup>11</sup> (100 N), held constant for 2 s, and then linearly decreased back to 0. For each joint, with the joint surface intact (the baseline condition), contact stresses in the medial compartment were first measured at five flexion angles ranging from  $125^\circ$  to  $145^\circ$  in  $5^\circ$  increments. Subsequently, a 2-mm diameter osteochondral defect was created (the defect condition) in a manner identical to that in the survival experiment, and the above-described contact stress measurement protocol was repeated. Contact stress data captures at the flexion angle showing the greatest contact circumferentially around the defect region were chosen for quantitative analysis. Films were digitized at a resolution of 118 pixels/cm and were analyzed using a purpose-written program implemented in MATLAB (MathWorks<sup>™</sup>, Inc., Natick, MA). These analyses used a calibration curve generated using a 6.35 mm diameter rigid platen and eight known stress levels, to convert the pixel intensity values to peak contact stress values. This analysis program identified the outline(s) of the contact patch (based on an intensity threshold), and then calculated the total contact area, the peak contact stress value, and the maximal sagittal- and coronal-direction spans of the contact patch (Fig. 3B).

The immediate effects of defect creation on sagittal-plane stability were assessed in a manner identical to that described for the survival animal experiment. Each knee, with the primary weight-bearing region of its medial femoral surface being exposed by means of posterior arthrotomy, was tested with the articular surface intact (baseline) and then immediately after defect creation.

### Statistical Analysis

In the survival experiment, because the number of animals for each combination of treatment (incongruous injury vs. sham surgery control) and test period (8 weeks vs. 16 weeks) was relatively small ( $n = 10$ ), a nonparametric test (the Wilcoxon rank-sum test) was used to test for equality of treatment means, using the pooled 8- and 16-week data ( $n = 20$ , per group). This test was applied individually to the four respective surface histological scores and to the stability measure. Exploratory comparisons were performed between test periods ( $n = 10$  per sub-group) within each treatment group, again using the rank-sum test. Data from cadaver loading tests (contact mechanics and stability) were compared between the baseline and defect conditions, again using the Wilcoxon signed-rank test. Because of the small sample size (hence low power) and to avoid inflation of the overall type I error rate, these tests were considered to be exploratory. All tests were performed using a significance level of alpha set at 0.05.

### RESULTS

In histological analysis for the survival study (Fig. 4), comparisons between treatment groups (for which the data from the 8- and 16-week animals were pooled) indicated that the incongruous injury group had cartilage degeneration (histological scores significantly higher than in the sham surgery control group) for the medial femoral surface ( $p < 0.0001$ ), the medial tibial surface ( $p < 0.0001$ ), and the lateral femoral surface ( $p = 0.0011$ ). For the medial tibial surface, degeneration reached the middle- to deep-zone (HHGS  $\geq 4$ ) in most cases, in both the 8- and 16-week animals. For the medial femoral surface, similar severe degeneration was identified in the 16-week animals (7 of 10), with the

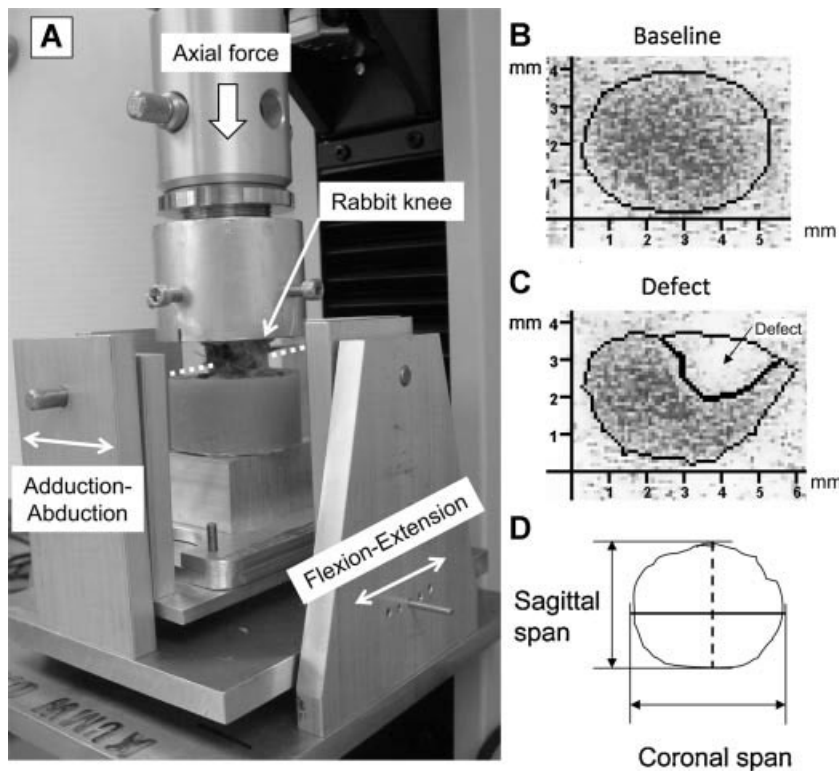


**Figure 3.** (A) Custom loading fixture for the contact mechanics test. The sagittal-plane position (flexion-extension) of the rabbit knee was adjustable in  $5^\circ$  increments. The coronal-plane rotation (ad-abduction) about the axis passing through the center of joint (dotted line) was unrestricted. (B and C) Representative digitized Fujifilm images that indicate contact stress distribution in the medial compartment before (baseline) and contact stress redistributed after defect creation (defect). (D) The longest spans of the contact patch in the sagittal direction (dashed black line) and in the coronal direction (solid black line) were registered.

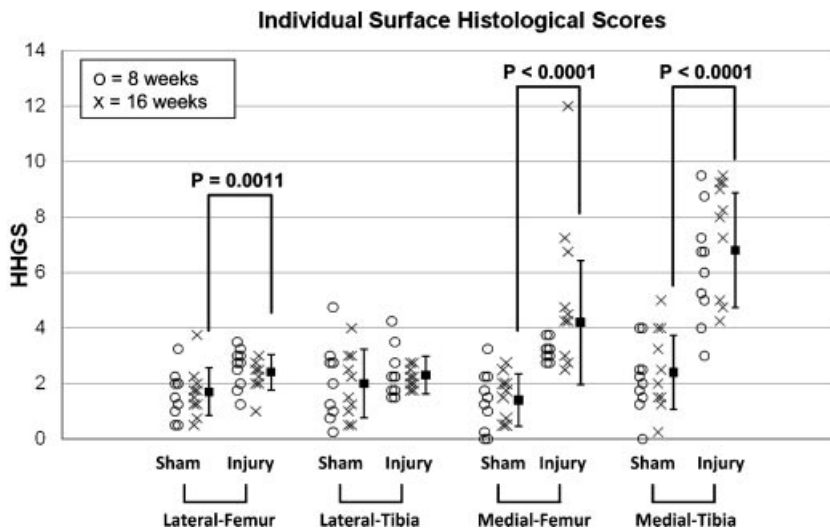


**Figure 4.** HHGS scores for each individual animal are plotted, along with the mean values (from both 8- and 16-week animals). The dispersion bars indicate standard deviations.

difference between the time-period sub-groups not being significant ( $p = 0.072$ ). For the lateral femoral surface, degenerative changes were relatively mild ( $HHGS < 4$ ) in all cases. Appreciable remodeling of bone and cartilage in the defect region (reaching the level of articular surface) was not identified in any knees in the incongruous injury group.

In the survival animal stability test (Fig. 5A), the NZL in the incongruous injury group (including both 8- and 16-week animals) was significantly longer ( $p = 0.014$ ) than in the sham surgery group, indicating that the incongruous knees had increased sagittal-plane laxity at the time of euthanasia. The mean increase with respect to the sham surgery group was 20%. No significant difference between time periods was evident. By contrast, in cadaver experimentation (Fig. 5B), sagittal-plane stability remained nearly equivalent before versus after defect creation ( $p = 0.94$ , RMS difference = 7.4%).

In the cadaver contact mechanics test, changes in the shape of contact patch (Fig. 3B) associated with defect creation showed significant increases of coronal and

sagittal spans ( $p = 0.031$  for both, Fig. 6). This occurred, however, without an accompanying increase in engaged contact area ( $p = 0.47$ ), suggesting that contact stresses were simply shifted from the defect area onto the adjacent regions of the joint surface. Slight increase (up to +23.5%) of peak contact stress value with defect creation occurred in six of seven specimens ( $p = 0.078$ ).

**DISCUSSION**

The present study explored whole-organ cartilage responses from localized osteoarticular injury in the rabbit knee in vivo, for the first time simultaneously with the associated changes in joint mechanics. Use of the posterior surgical approach allowed creating an isolated osteochondral defect in the most heavily weight-bearing posterior region of the medial femoral condyle, without damaging the surrounding cartilage. This surgical insult necessarily involved intraarticular bleeding from incised capsule and bone marrow, and cartilage is sensitive to exposure to blood.<sup>12,13</sup> However, this hemoarthrosis is actually consistent with clinical

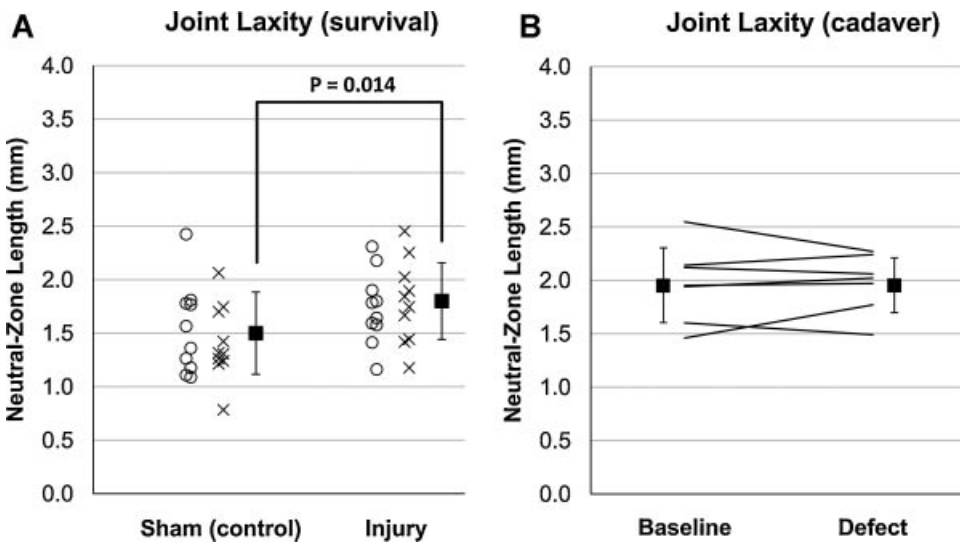


**Figure 5.** (A) Survival animal stability results. Individual-animal data are plotted for the sham surgery (control) and incongruous injury groups, along with the mean and standard deviation for each group (from both 8- and 16-week animals). (B) Cadaver specimen stability results. Corresponding individual-specimen data are plotted before (baseline) and after defect creation, along with the mean and standard deviation for each condition.

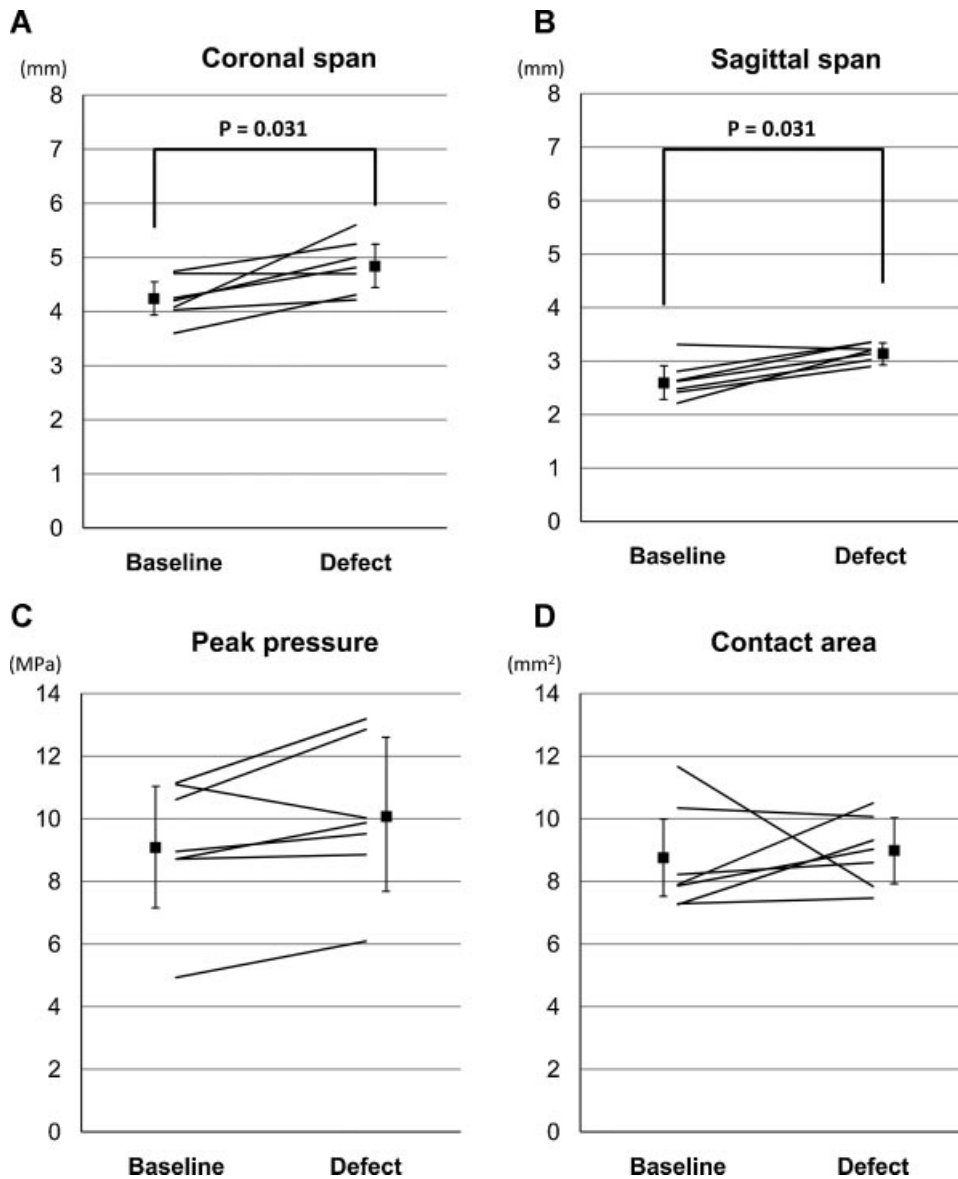


**Figure 6.** Cadaver specimen contact stress results. Corresponding individual-specimen data are plotted before (baseline) and after defect creation, along with the mean and standard deviation for each condition.

conditions after traumatic osteoarticular injuries or surgical intervention for them. The survival model, which involved a relatively small solitary osteoarticular injury on the medial femoral surface (a 2-mm full-thickness osteochondral defect in the weight-bearing region), exhibited appreciable cartilage degeneration in the medial compartment, both near the femoral defect itself and on the opposing tibial surface. In addition to this local degeneration, modest but significant degenerative changes in cartilage histology were identified at a remote location (on the lateral femoral surface). As hypothesized, a localized osteoarticular injury influenced whole-joint cartilage conditions. This is different from whole-joint arthritis secondary to whole-joint insult, as in the murine knee fracture model of Furman et al.<sup>14</sup> By implication, there were organ-level mechanism(s) by which a localized osteoarticular injury induced propagation of cartilage degeneration to the whole-joint level.

In a previous horse knee model of osteoarticular injury,<sup>15</sup> a larger diameter (9–21 mm) circular defect created on the medial femoral condyle caused cartilage degeneration on the opposing medial tibial plateau surface, with the degrees of degeneration increasing with defect size. In a rabbit knee model,<sup>16,17</sup> incongruous osteoarticular injury on the medial femoral condyle was modeled by creating a 3-mm wide longitudinal osteochondral fragment through an anterior arthrotomy, with the fragment fixed at a 2- or 5-mm proximally displaced “step-off” position. Joints with a 5-mm step-off developed degeneration across the whole joint, including the opposing medial tibial cartilage,<sup>17</sup> though such a phenomenon was not evident with the 2 mm step-off.<sup>16</sup> However, since the femoral surface accessible through an anterior arthrotomy is typically the inferior aspect rather than posterior, success in positioning the step-off in the primary weight-bearing surface may have been different between groups. Observations in those models

are consistent with the present study, in that femoral incongruity caused degeneration on the opposing tibial surface. However, the percentage of the weight-bearing surface having a step-off appears to be smaller in the present study (with a 2-mm circular defect) than in those models.

In the cadaver contact mechanics test, the immediate effects of defect creation did not involve dramatic elevation of peak local contact stress, as previously documented in a canine osteochondral defect knee model.<sup>2</sup> However, the morphology of the contact patch changed significantly with defect creation, indicating that the incongruous injury knees in the survival experiment must have had similarly aberrant contact mechanics in the medial compartment. At a microscopic level, cartilage opposing a defect surface is subjected to supra-physiologic deformation associated with the stress gradient at the boundary between contact and non-contact regions.<sup>18</sup> During joint motion, cartilage at that boundary is presumably also subjected to a supra-physiologically high rate of deformation. Given that chondrocytes are very sensitive to loading rate,<sup>19–22</sup> such abnormal dynamic loading plausibly explains the medial compartmental degeneration in the survival experiment. In addition, redistribution of contact stresses from the weight-bearing region to a less loaded peripheral region may have affected the cartilage local mechanical milieu, causing adverse long-term effects.<sup>23</sup> These dynamic mechanisms may have caused the compartment degeneration accompanying the relatively small osteochondral defect.

Stability testing in the survival study demonstrated that the rabbit knees with the osteoarticular injury had modestly increased laxity at the time of euthanasia. However, such laxity was not identified in the rabbit cadaver stability test. Presumably, the increased laxity in the survival study therefore developed secondarily during the testing period, by biologically mediated mechanisms such as collagen fiber weakening caused by inflammatory cytokines.<sup>24,25</sup> The extra surgical insult in the incongruous injury knees (i.e., defect creation) may have caused stronger acute inflammation compared to the control knees with an otherwise identical surgical procedure. The resulting joint instability, along with abnormalities in the joint kinematics associated with the aberrant medial compartment contact mechanics, probably contributed to whole-joint degenerative changes in cartilage histology, by causing instability events involving deleteriously high-rate cartilage loading.<sup>5</sup> Besides such biomechanical factors, an organ-level biologic response to acute (surgical) osteoarticular injury likely also affected cartilage throughout the joint. Custers et al.,<sup>26</sup> who reported remote-site cartilage degeneration in the rabbit knees with a 3.5-mm medial femoral defect (created through an anterior arthrotomy at an inferior location rather than posterior), linked the mechanism of remote degeneration with an organ-level biologic response as proposed by Saris et al.<sup>27</sup> According to this concept, loss of physiologic equilibrium between the

structures in a synovial joint following an injury leads to abnormal production of a myriad of intra-articular factors, such as inflammatory cytokines or cellular components, which affect the entire joint. Therefore, the remote-site degenerative changes were probably secondary to incongruity-associated biomechanical abnormalities, in concert with acute traumatic disturbance of organ-level physiologic homeostasis of the joint.

A limitation of this study was that cartilage degeneration was quantified purely with histological indices, which depend on subjective observer judgment. However, both observers repeated their measurements in a blinded fashion, and inter-observer and intra-observer reliabilities were high ( $r > 0.9$  for both). The “whole-joint” histological evaluation was performed only in the femorotibial joints; the patellofemoral joint was not included. Lack of means to measure local inflammation precluded studying the contributions of inflammatory biological responses to the reported changes in cartilage histology and joint laxity. Further investigation is needed to clarify the mechanisms of the remote-site cartilage changes and increased joint laxity observed in the survival study. Finally, no significant differences were detected between specimens observed at 8 versus 16 weeks. Lack of significant time dependence may have been due to the two time points having been too close together or to insufficient power to detect a meaningful effect size (the power was  $< 33\%$  for detecting a difference as large as a 0.5-fold standard deviation if the distributions were normally distributed). The lack of progression over the second 8 weeks of the experiment may also have been influenced by the rabbits being confined to cage activity, as opposed to moving in their natural environment.

In conclusion, the short- to mid-term whole-joint effects of an isolated localized osteoarticular injury in the weight-bearing surface of the rabbit knee medial femoral condyle involved degenerative changes in cartilage histology that occurred predominantly—but not exclusively—in the medial compartment. The mechanical data demonstrated that the accompanying localized incongruity involved the onset of biomechanical abnormality consistent with causing cartilage degeneration. Presumably, the pathomechanisms operating in this animal model also contribute to development of post-traumatic OA after human osteoarticular injuries.

## ACKNOWLEDGMENTS

This research was supported by research grants from the CDC (R49 CCR721745) and the NIH (5 P50 AR048939 and 5 P50 AR055533).

## REFERENCES

1. Buckwalter JA, Brown TD. 2004. Joint injury, repair, and remodeling: roles in post-traumatic osteoarthritis. *Clin Orthop Relat Res* 423:7–16.
2. Brown TD, Pope DF, Hale JE, et al. 1991. Effects of osteochondral defect size on cartilage contact stress. *J Orthop Res* 9:559–567.

3. Koh JL, Wirsing K, Lautenschlager E, et al. 2004. The effect of graft height mismatch on contact pressure following osteochondral grafting: a biomechanical study. *Am J Sports Med* 32:317–320.
4. McKinley TO, Tochigi Y, Rudert MJ, et al. 2008. The effect of incongruity and instability on contact stress directional gradients in human cadaveric ankles. *Osteoarthritis Cartilage* 16:1363–1369.
5. McKinley TO, Tochigi Y, Rudert MJ, et al. 2008. Instability-associated changes in contact stress and contact stress rates near a step-off incongruity. *J Bone Joint Surg Am* 90:375–383.
6. Mansour JM, Wentorf FA, Degoede KM. 1998. In vivo kinematics of the rabbit knee in unstable models of osteoarthritis. *Ann Biomed Eng* 26:353–360.
7. Newton PO, Woo SL, MacKenna DA, et al. 1995. Immobilization of the knee joint alters the mechanical and ultrastructural properties of the rabbit anterior cruciate ligament. *J Orthop Res* 13:191–200.
8. Heiner AD, Rudert MJ, McKinley TO, et al. 2007. In vivo measurement of translational stiffness of rabbit knees. *J Biomech* 40:2313–2317.
9. Pritzker KP, Gay S, Jimenez SA, et al. 2006. Osteoarthritis cartilage histopathology: grading and staging. *Osteoarthritis Cartilage* 14:13–29.
10. Mankin HJ, Dorfman H, Lippiello L, et al. 1971. Biochemical and metabolic abnormalities in articular cartilage from osteoarthritic human hips. II. Correlation of morphology with biochemical and metabolic data. *J Bone Joint Surg Am* 53:523–537.
11. Gushue DL, Houck J, Lerner AL. 2005. Rabbit knee joint biomechanics: motion analysis and modeling of forces during hopping. *J Orthop Res* 23:735–742.
12. Hooiveld M, Roosendaal G, Vianen M, et al. 2003. Blood-induced joint damage: longterm effects in vitro and in vivo. *J Rheumatol* 30:339–344.
13. Hooiveld M, Roosendaal G, Wenting M, et al. 2003. Short-term exposure of cartilage to blood results in chondrocyte apoptosis. *Am J Pathol* 162:943–951.
14. Furman BD, Strand J, Hembree WC, et al. 2007. Joint degeneration following closed intraarticular fracture in the mouse knee: a model of posttraumatic arthritis. *J Orthop Res* 25:578–592.
15. Convery FR, Akeson WH, Keown GH. 1972. The repair of large osteochondral defects. An experimental study in horses. *Clin Orthop Relat Res* 82:253–262.
16. Lefkoe TP, Walsh WR, Anastasatos J, et al. 1995. Remodeling of articular step-offs. Is osteoarthritis dependent on defect size? *Clin Orthop Relat Res* 314:253–265.
17. Lefkoe TP, Trafton PG, Ehrlich MG, et al. 1993. An experimental model of femoral condylar defect leading to osteoarthritis. *J Orthop Trauma* 7:458–467.
18. Braman JP, Bruckner JD, Clark JM, et al. 2005. Articular cartilage adjacent to experimental defects is subject to atypical strains. *Clin Orthop Relat Res* 430:202–207.
19. Chen CT, Burton-Wurster N, Lust G, et al. 1999. Compositional and metabolic changes in damaged cartilage are peak-stress, stress-rate, and loading-duration dependent. *J Orthop Res* 17:870–879.
20. Lee DA, Bader DL. 1997. Compressive strains at physiological frequencies influence the metabolism of chondrocytes seeded in agarose. *J Orthop Res* 15:181–188.
21. Morel V, Quinn TM. 2004. Cartilage injury by ramp compression near the gel diffusion rate. *J Orthop Res* 22:145–151.
22. Sah RL, Kim YJ, Doong JY, et al. 1989. Biosynthetic response of cartilage explants to dynamic compression. *J Orthop Res* 7:619–636.
23. Andriacchi TP, Koo S, Scanlan SF. 2009. Gait mechanics influence healthy cartilage morphology and osteoarthritis of the knee. *J Bone Joint Surg Am* 91:95–101.
24. Kumar D, Fung W, Moore RM, et al. 2006. Proinflammatory cytokines found in amniotic fluid induce collagen remodeling, apoptosis, and biophysical weakening of cultured human fetal membranes. *Biol Reprod* 74:29–34.
25. Qi J, Fox AM, Alexopoulos LG, et al. 2006. IL-1beta decreases the elastic modulus of human tenocytes. *J Appl Physiol* 101:189–195.
26. Custers RJ, Creemers LB, van Rijen MH, et al. 2009. Cartilage damage caused by metal implants applied for the treatment of established localized cartilage defects in a rabbit model. *J Orthop Res* 27:84–90.
27. Saris DB, Dhert WJ, Verbout AJ. 2003. Joint homeostasis. The discrepancy between old and fresh defects in cartilage repair. *J Bone Joint Surg Br* 85:1067–1076.